Journal of Soils and Sediments (2020) 20:272–283
https://doi.org/10.1007/s11368-019-02408-1

SOILS, SEC 2 • GLOBAL CHANGE, ENVIRON RISK ASSESS, SUSTAINABLE LAND USE • RESEARCH ARTICLE

Soil particle-size distribution and aggregate stability of new reconstructed purple soil affected by soil erosion in overland flow

Feng-Lin Zuo[1,2] · Xiao-Yan Li[1,2] · Xiao-Fan Yang[1,2] · Yang Wang[1,2] · Yu-Jun Ma[1,2,3] · Yu-Han Huang[4] · Chao-Fu Wei[5]

Received: 25 October 2018 / Accepted: 15 July 2019 / Published online: 9 August 2019

Abstract

Purpose Artificial soil erosion caused by engineering practices is becoming increasingly severe worldwide. However, little is known about the change of soil structure of new reconstructed purple soil after erosion in the hilly areas of Southwest China. This study aims to analyze the effects of erosion on the soil particle-size distribution (PSD) and aggregate stability of new reconstructed purple soil in the overland flow under different flow discharges, slope lengths, and slope positions.

Materials and methods A series of field scouring experiments was conducted. Flow discharges of 5, 15, and 30 L/min were applied in the new reconstructed purple soil plots with different slope lengths (5, 10, 20, 30, 40, and 50 m). Sediment samples were collected in 550-mL bottles. Soil sampling was conducted from the 0–10-cm layers before and after the field scouring experiments. In the laboratory, the pipette method was used to measure the soil PSD and microaggregates. The macroaggregates were determined by the dry and wet sieving method.

Results and discussion Silt particles were eroded most at 30 L/min, by 2.11%. The average maximal reduction rate of the mean weight diameter of soil aggregates (MWD) was 20.23% at 15 L/min. Clay loss was maximal at 1.04%, and the average maximal increasing rate of the > 0.25 mm percentage of aggregate disruption ($PAD_{0.25}$) was 0.86% at 5 L/min. The silt and MWD maximally decreased by 7.72% and 1.86%, and the maximal sand and $PAD_{0.25}$ increased by 16.70% and 25.18%, which were all observed in the 10-m plot. The percentage of soil aggregates destroyed by the change in the MWD was − 14.32% on the upslope. Silt sediment showed an increasing rate of 6.36% and microaggregate destruction showed a decreasing rate of 13.00% on the middle slope. Microaggregates and clay particles were mainly deposited on the lower slope and the reduction rates of the silt and sand content were smaller than those on the middle slope.

Conclusions The effects of erosion on the soil PSD and aggregate stability of new reconstructed purple soil in the overland flow under different flow discharges, slope lengths, and slope positions were obviously different. Soil and water conservation measures should be effectively implemented on the upper slope and a slope length of 10-m soil. The soil PSD and MWD could be used as parameters for prediction of soil erosion on new reconstructed purple soil.

Responsible editor: Saskia Keesstra

✉ Chao-Fu Wei
weicf@swu.edu.cn

[1] State Key Laboratory of Earth Surface Processes and Resource Ecology, Faculty of Geographical Science, Beijing Normal University, Beijing 100875, China

[2] School of Natural Resources, Faculty of Geographical Science, Beijing Normal University, Beijing 100875, China

[3] Present address: School of Geography and Planning, Sun Yat-sen University, Guangzhou, China

[4] College of Water Resources and Civil Engineering, China Agricultural University, Beijing 100083, China

[5] College of Resources and Environment, Southwest University, Chongqing 400716, China

Keywords New reconstructed soil · Purple soil · Soil erosion · Soil structure · Scouring experiment

1 Introduction

Artificial soil erosion caused by engineering measures has become more severe worldwide (Cerdà et al. 2007; Peng et al. 2014; Chen et al. 2016). Compared with the erosion process of natural soil, that of sloped farmland soil after farmland consolidation engineering is more complex (Sklenicka 2006). The new reconstructed soil which exhibits unstable behavior immediately after the implementation of farmland consolidation projects is in the restoration (RP) period (Yu et al. 2010). Thus, the soil erosion of the

new reconstructed soil should be fully considered and investigated. Existing research has found that the effects of farmland consolidation engineering on the soil structural properties were significant (Wang et al. 2011). For example, the sand and aggregate disruption (PAD) was significantly reduced, and the silt, clay, and mean weight diameter of the soil aggregates (MWD) increased significantly (Ramos et al. 2007; Liu et al. 2015). The soil physical quality was much lower and most unstable 6~12 months after land consolidation (Xu et al. 2009; Curtaz et al. 2015). However, the effects of erosion on the soil structure of new reconstructed soil are rarely studied. New reconstructed soil is widespread in the hilly areas of Southwest China (Liu 2015). Particularly, purple soil corresponds to Regosols according to the FAO/UNESCO classification system (FAO/Unesco 1988), which occurs mainly in Chongqing and Sichuan of China which easily eroded and serve as the main sediment source in the Three Gorges Reservoir area (Xie et al. 2005). Acid purple soil contains more montmorillonite in which the stability of soil aggregates is poorer than other Regosols soils (Wakindiki and Ben–Hur 2002), because the parent sedimentary rock environment of the purple soil belonging to Shaxi Miao Formation is a river with relatively dry conditions (Wei et al. 2006; He et al. 2009). Previous studies have evidently shown the characteristics of the soil loss and hydrodynamic parameters of new reconstructed purple soil during the erosion process (Zuo et al. 2018). The erosion resistance of new reconstructed purple soil is weak due to its high gravel content, deteriorating physical properties, and low organic matter content (Wei et al. 1994; Wei et al. 2000). Hence, the effects of erosion on the soil structure of new reconstructed purple soil are considered to be unique.

The soil particle-size distribution (PSD) and soil aggregate stability have been demonstrated to be the key factors controlling soil erosion (Fiès and Bruand 1998). In particular, there are contradictive views on the effect of the soil PSD and aggregate stability on erosion. High silt and (or) clay contents could lead to high soil erosion (Ampontuah et al. 2006; Piccarreta et al. 2006), which is opposite of the conclusion of Wu et al. (2017). Numerous studies have demonstrated that fine particles (such as silt and fine clay) are more easily eroded by runoff than coarse materials (Starr et al. 2000; Refahi 2000; Nadeu et al. 2010). Many studies have revealed negative relationships between aggregate stability and soil erosion, for instance, in the aggregate stability indexes of the water-stable aggregate content, macroaggregates, microaggregates, and MWD (Refahi 2000; Fox et al. 2004; Thomaz 2018). However, microaggregates, which are < 0.05-mm aggregates and (or) 0.5~1- and 0.25~0.5-mm soil aggregates, were preferentially transported in the erosion process (Shen et al. 2008; Hao et al. 2019). However, most studies focused on the changes of soil PSD and aggregate stability after erosion of stable soil without further investigation on the unstable soil. Thus, the effects of erosion on the soil PSD and aggregate stability of new reconstructed purple soil should be quantified in detail to effectively carry out soil and water conservation and modeling.

The runoff, slope length, and slope position are commonly used to describe the degree of soil erosion (Meyer and Monke 1965; Liu et al. 2000; Tian et al. 2015). The influence of rainfall or runoff on the aggregate size is debatable. On the one hand, the rainfall intensity might play a negative role in the erosion process, and the detach ability of macroaggregates has been shown to increase with the increase in rainfall (Shen et al. 2008; Lu et al. 2016; Wu et al. 2017). On the other hand, increasing rainfall might cause the MWD to first decrease and then increase in the sheet flow (Hao et al. 2019). When the rainfall was greater than a certain threshold, the macroaggregates (> 0.25 mm) disintegrated seriously (Wang et al. 2014; Hao et al. 2019). Moreover, a large proportion of the fine soil aggregate components of the runoff was found when rainfall was light (López-Tarazón et al. 2010; Shi et al. 2012) and coarser particles were associated with higher stream power (Asadi et al. 2011). Many previous studies have also found that the erosion amount decreased, increased, or fluctuated upon increasing the slope length (Stomph et al. 2002; Liao et al. 2008; Kara et al. 2010). It was also found that the upslope area was erosive area, while mid-slope and lower slope areas were depositional sites. For example, Kosmas et al. (2001) found that massive amount of clay was deposited in the lower slope position. Chen et al. (2010) reported that clay and silt decreased in upslope areas, clay and silt increased in mid-slope areas, and clay and sand increased in lower slope areas. Wang et al. (2018) indicated that the macroaggregate contents at depositional sites were higher than those in eroded slope farmland areas. In contrast, Ampontuah et al. (2006) found that the clay and fine silt contents on upper slope were higher than those in lower slope samples. Therefore, the effects of the overland flow discharge, slope length, and slope position on soil erosion should be systematically studied, especially through field experiments on new reconstructed purple soil.

To bridge the knowledge gaps, this study sought to analyze the effects of erosion on the soil structure of new reconstructed purple soil in overland flow under different flow discharges, slope lengths, and slope positions. The current study specifically aimed to (i) measure the changes of the soil PSD and aggregate stability of new reconstructed purple soil in overland flow under different flow discharges, slope lengths, and slope positions and (ii) establish the relationship between the most correlative structure index and soil erosion. The results of this study could provide important parameters for predicting soil erosion through monitoring soil structural variables which can be used to control the erosion of new reconstructed slope soil in hilly areas with purple soils.

2 Material and methods

2.1 Experimental sites

This study was conducted at the national purple soil monitoring base of Southwest University, Beibei District, Chongqing (106° 26′ E, 30° 26′ N, and 230 m a.s.l.) (Fig. 1). The study site is located in the transition zone between the Qinghai-Tibet Plateau and the middle reaches of the Yangtze River. The topography of the study site is characterized by the Beibei Syncline of the parallel mountain ridge and valley region in east Sichuan. The area has a humid subtropical monsoonal climate with a mean annual temperature of 18.3 °C and an average annual precipitation of 1105 mm. The soil type is purple soil developed from the gray-brown-purple sandy mudstone of the Shaximiao Formation (J_2s) of the Jurassic system. The soil properties before reconstruction are listed in Table 1.

At the experimental site, farmland with a 20° slope was selected, and the slope angle was reduced to 10° by converting the sloped land into terraces (Chongqing Land Development and Consolidation Project Construction Standard 2007). The farmland consolidation was performed according to the following steps. First, a 20-cm topsoil layer was stripped from the original slope farmland. Second, engineering measures including deep excavation, refilling, land-reshaping, and leveling were implemented. Rectangular experimental plots were established without fertilization and crops. The slope length was designed to be 5, 10, 20, 30, 40, or 50 m (Fig. 1). The width and depth of the plots were 2 m and 0.6 m, respectively. The plots were separated by a 0.2-m-wide cement ridge built on the parent material. The bottoms of the plots contained natural soil parent material. The field scouring experiments were carried out immediately after completion of the farmland consolidation. Before the field scouring

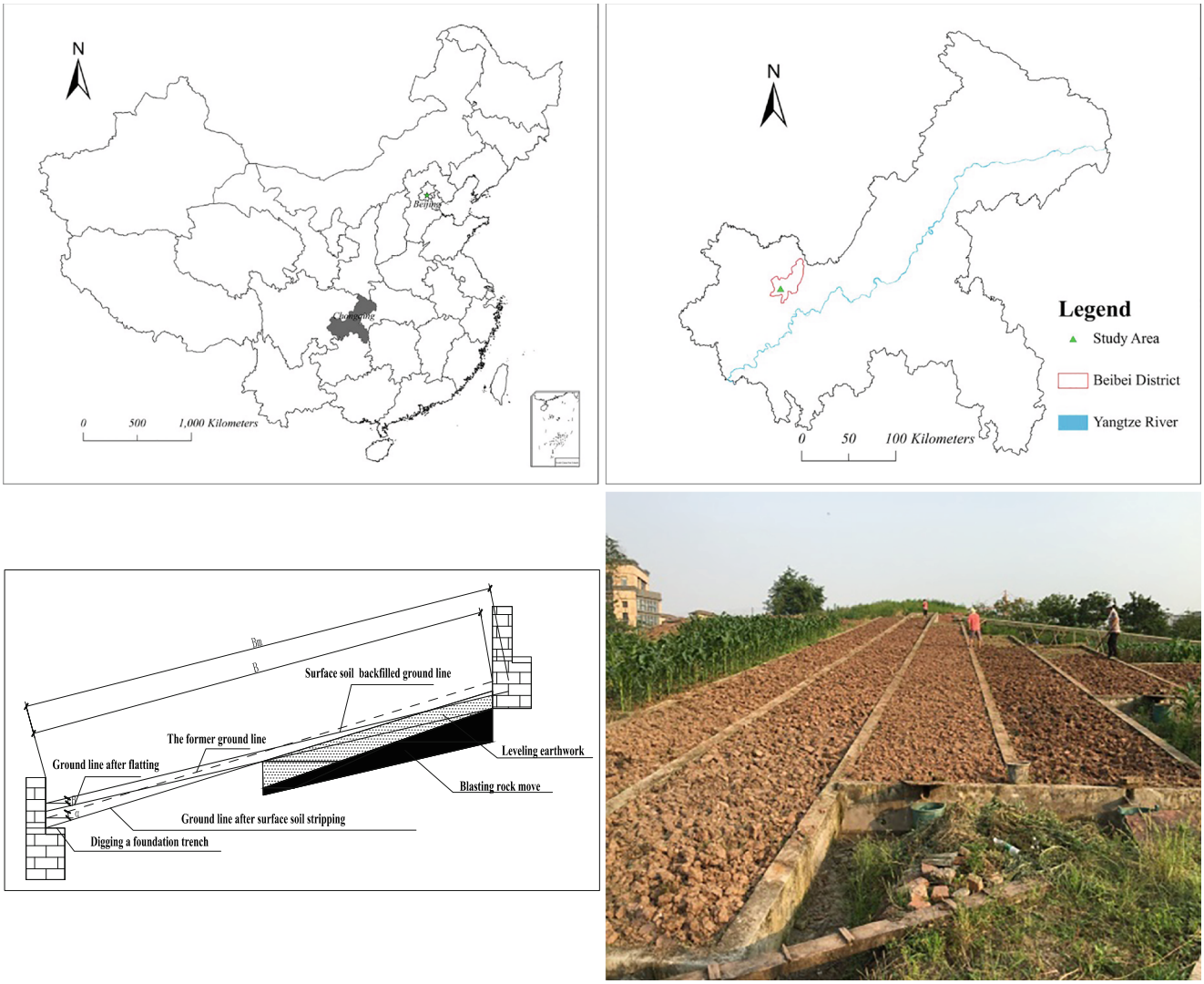

Fig. 1 Layout of the experiment plots at Southwest University, Chongqing

Table 1 Soil properties before the farmland consolidation engineering at Southwest University, Chongqing

Position	Depth (cm)	Bulk density (g/cm^3)	pH	Soil organic matter (g/kg)	Clay (%)	Silt (%)	Sand (%)
Upper slope	0~20	1.43	6.87	12.60	16.14	39.04	44.82
	20~40	1.54	7.21	5.51	19.78	39.49	40.73
Middle slope	0~20	1.30	5.60	16.50	17.90	41.27	40.83
	20~40	1.61	6.20	8.26	22.64	42.15	35.22
Lower slope	0~20	1.41	5.59	16.04	22.17	40.29	37.54
	20~40	1.58	6.22	12.38	20.14	43.92	35.94

experiments, approximately 15 cm of topsoil in the experimental plots was loosened (equivalent to the farmland tillage depth) to implement tillage similar to that generally used in agricultural land.

2.2 Design and measurements of the field scouring experiment

The field scouring experimental design is shown in Fig. 2. Based on the observation data collected from local runoff plots, topographical conditions, and maximum amount of runoff (Liu 2015), the simulated flow discharges on the new reconstructed purple soil were 5, 15, and 30 L/min. Eighteen field scouring experiments were conducted in this study; however, there was no runoff in the 40-m and 50-m plots at 5 L/min. A storage bucket was used to supply the water, and the overflow chute was placed horizontally at the top of the test area, such that the surface water flow remained sheet-like and uniformly distributed. The top of the overflow chute was equipped with a faucet to regulate the flow discharge. A pump and flowmeter were used to provide stable flow discharge. The plots were raked flat and allowed to stand for about a week before the field scouring experiments to prevent the influence of the surface roughness and initial soil moisture content on the experimental results. The soil was saturated for 12 h before the field scouring experiments. The experiment was started when the error between the actual and designed flow discharges was less than 5%. The flow supply was stopped until the runoff was steady. The runoff bucket was placed under the collecting tank to collect the surface runoff when surface runoff was generated. After flow supply stopped, it continued to receive the surface runoff until the end of the runoff production. Sediment samples were collected in 550-mL bottles at 1-min intervals for the first 10 min and at 3-min intervals thereafter. The sediment yield was calculated by the drying method (105 °C). We selected three slope positions (upper, middle, and lower slope) in the slope length of the 5-, 10-, 20-, 30-, 40-, and 50-m plots. Three topsoil (0~10 cm) samples for replication were collected from each of the slope positions before and after the field scouring experiments of the three flow discharges. The sampling points were randomly selected from areas eroded by runoff. Although there was no runoff in the 40-m and 50-m plots, the soil structural properties changed at different slope positions, and we also collected soil samples from these plots. The soil samples were collected for further determination of the soil PSD and soil aggregate stability. The soil properties before the field scouring experiment are shown in Table 2.

The erosion rate is the amount of sediment produced on the slope per unit time and can be obtained by

$$E_r = \frac{M}{t} \tag{1}$$

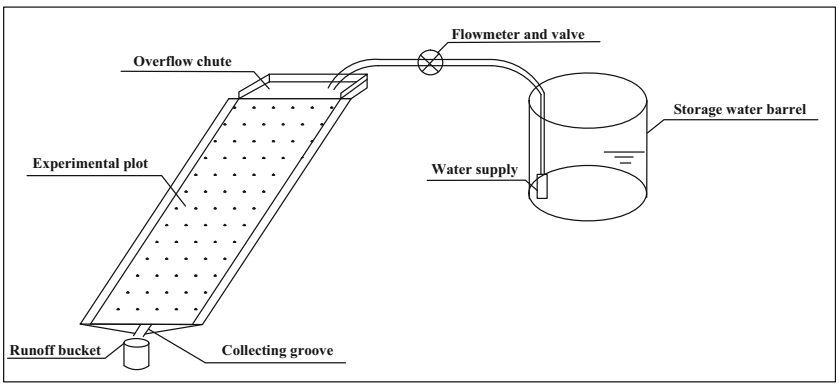

Fig. 2 Layout of the experimental setup

Table 2 Mean values, standard deviation, and coefficients of variation (CVs) of the soil PSD, > 0.25-mm aggregate destruction rate ($PAD_{0.25}$), soil mean weight diameter (MWD), and < 0.02-mm soil aggregation degree (*Y*) for each plot before runoff scouring

Slope length (m)	The soil particle-size distributions (PSD)			$PAD_{0.25}$ (%)	MWD	*Y* (%)
	Clay (%) (<0.002 mm) (CV)	Silt (%) (0.05~0.002 mm) (CV)	Sand (%) (2~0.05 mm) (CV)			
5	30.18 ± 0.35^{a}	41.42 ± 2.41^{ab}	28.39 ± 2.67^{ab}	96.42 ± 0.2^{a}	114.45 ± 24.94^{ab}	17.10 ± 7.69^{a}
	0.01	0.06	0.09	0.00	0.22	0.45
10	29.78 ± 3.43^{a}	43.05 ± 1.71^{a}	27.16 ± 2.44^{b}	95.48 ± 0.77^{b}	154.19 ± 40.35^{a}	18.04 ± 1.16^{a}
	0.12	0.04	0.09	0.01	0.26	0.06
20	29.11 ± 2.13^{a}	39 ± 0.87^{ab}	31.89 ± 2.37^{ab}	96.82 ± 0.24^{a}	159.95 ± 6.41^{a}	29.66 ± 28.31^{a}
	0.07	0.02	0.07	0.01	0.04	0.95
30	28.68 ± 0.93^{a}	37.8 ± 5.59^{ab}	33.52 ± 5.03^{ab}	96.98 ± 0.33^{a}	131.20 ± 24.38^{ab}	21.17 ± 2.66^{a}
	0.03	0.15	0.15	0.00	0.19	0.13
40	27.12 ± 3.63^{a}	36.69 ± 3.01^{b}	36.19 ± 6.64^{a}	96.63 ± 0.22^{a}	99.35 ± 20.33^{b}	11.51 ± 2.94^{a}
	0.13	0.08	0.18	0.00	0.20	0.26
50	29.99 ± 2.38^{a}	39.85 ± 2.6^{ab}	30.16 ± 4.69^{ab}	96.46 ± 0.62^{a}	122.50 ± 20.37^{ab}	21.08 ± 9.13^{a}
	0.08	0.07	0.16	0.00	0.17	0.43

Different letters indicate significant differences between different plots

where E_r is the erosion rate (g/min), *M* is the sediment weight in the 550-mL bottles (g), and *t* is the sampling time (min).

2.3 Measurement of the soil particle-size distribution and soil aggregate

In the laboratory, the soil samples were naturally dried and divided into two equal parts. The first sample was sieved through 2-mm mesh to analyze the soil PSD distribution, microaggregates, and pH, whereas the second sample was used to assess the soil aggregates. The properties of each soil sample were determined in triplicate. Soil pH was determined by potentiometry in water using a 1:5 soil-water extract. The pipette method with Na hexametaphosphate after soil organic matter (SOM) oxidation with H_2O_2 was used to measure the soil PSD (Zheng 2013). Soil microaggregates were determined using the pipette method without the removal of the SOM. According to the soil texture classification system of the USDA, the soil particles were divided into sand (2~0.05 mm), silt (0.05~0.002 mm), and clay (< 0.002 mm). The size distribution of the dry-stable aggregates was determined by the dry sieving method. Soil samples were placed on a stack of sieves (10, 7, 5, 3, 2, 1, 0.5, and 0.25 mm) and vibrated for 10 min (SZH, Nanjing Soil Instrument Factory, China). The water-stable aggregates with a diameter of > 0.25 mm were analyzed by the conventional wet sieving method (TPF-100, Nanjing Soil Instrument Factory, China). Stacked sieves (5, 2, 1, 0.5, and 0.25 mm) were put into the water and moved up and down for 30 min at a frequency of 30 times/min (Oades and Waters 1991).

The soil aggregate size of 0.25 mm represents the boundary between macroaggregates and microaggregates (Six et al. 2000). The soil aggregate stability was indicated by the mean weight diameter of the soil aggregates (MWD), the > 0.25 mm percentage of aggregate disruption ($PAD_{0.25}$), and the degree of aggregation (*Y*) (Zhang et al. 2014). These values were calculated with Eqs. (2) to (4). The index Δ was considered to be the change in the soil structure affected by erosion in overland flow and was calculated as follows: Δ = (the indicator value after scouring − the indicator value before scouring) the indicator value before scouring.

$$\mathrm{MWD} = \sum_{i=1}^{6} x_i w_i \quad (2)$$

Table 3 The average erosion rates of new reconstructed purple soil under different slope lengths and flow discharges

	Flow discharge (L/min)	Slope length (m)					
		5	10	20	30	40	50
Average erosion rate (g/min)	30	81.44 ± 36.48	239.09 ± 160.98	26.98 ± 13.45	151.37 ± 92.07	16.96 ± 12.58	18.50 ± 16.30
	15	16.78 ± 18.76	121.21 ± 89.90	26.54 ± 7.08	4.05 ± 2.52	8.17 ± 5.88	8.63 ± 6.51
	5	1.11 ± 1.69	1.17 ± 0.89	12.05 ± 10.62	6.67 ± 4.54	–	–

Here, x_i is the mean diameter of each size class (< 0.25 mm, 0.25~0.5 mm, 0.5~1 mm, 1~2 mm, 2~5 mm, and > 5 mm), and w_i is the weight fraction of aggregates in size class i.

$$\mathrm{PAD}_{0.25} = \frac{(D_{0.25} - W_{0.25})}{D_{0.25}} \times 100\% \quad (3)$$

Here, $D_{0.25}$ is the > 0.25-mm dry-sieved aggregate content, and $W_{0.25}$ is the > 0.25-mm water-stable aggregate content.

$$Y = \frac{a' - b'}{b'} \times 100\% \quad (4)$$

Here, a' is the > 0.02-mm water-stable aggregate content, and b' is the > 0.02-mm mechanical composition.

3 Results

3.1 Characteristics of the soil particle-size distribution, soil aggregate stability, and erosion rates after farmland consolidation

The clay content was 16.14~22.17% and the silt and sand contents were 39.04~41.27% and 37.54~44.82%, respectively, before farmland consolidation (Table 1). The soil PSDs of the new reconstructed purple soil showed that the soil texture was clay loam with a high content of silt particles (36.69~43.05%) and that the silt content was maximal in the 10-m plot before runoff scouring (Table 2). Before runoff scouring, the MWD, $\mathrm{PAD}_{0.25}$, and Y of the new reconstructed purple soil were 99.35~159.95, 95.48~96.98%, and 11.51~29.66%, respectively, and the minimal $\mathrm{PAD}_{0.25}$ was 95.48% at 10 m (Table 3). The range of the average erosion rate was 1.11 (5 m, 5 L/min)~239.09 g/min (10 m, 30 L/min), as shown in Table 3. The partial correlation analysis revealed that the effects of the erosion rate on the flow discharge and slope length were significant ($r = 0.585$, $p < 0.05$ and $r = 0.561$, $p < 0.05$, respectively). The erosion rate increased with the increase in the flow discharge. The change in the erosion rate was not obvious with the increase in the slope length; however, it was the largest in the 10-m plot.

3.2 Effects of erosion on the soil structure in overland flow under different flow discharges, slope lengths, and slope positions

The ANOVA revealed that the effect of the flow discharge on the $\mathrm{PAD}_{0.25}$ was highly significant ($p < 0.01$) (Table 4) and that the slope length was significantly correlated with the MWD ($p < 0.05$). Other measured effects were not significant, but some trends in the changes after runoff souring were still observed (Fig. 3). The clay, silt, and sand variables before and after scouring are shown in Fig. 4 and Table 5. The MWD, $\mathrm{PAD}_{0.25}$, and Y variables before and after scouring are shown in Fig. 4 and Table 5. The response of the soil particle-size distribution (PSD) and soil aggregate stability to erosion in new reconstructed purple soil under different flow erosion rates was different. At 30 L/min, the maximal average reduction rate of silt was 2.11%, and sand particles showed an increase of 1.27%. The average ΔMWD and $\Delta\mathrm{PAD}_{0.25}$ were − 11.46% and 0.70%. The maximal average increase rate of Y was 27.64%. At 15 L/min, clay and silt were eroded simultaneously at average reduction rates of 0.80% and 1.00%, respectively, while the sand increased by 2.02%. The average reduction rate of the MWD was 20.23%. The average ΔY was 9.52%. At 5 L/min, the sand content increased by 1.11%. Clay and sand were removed at 1.04% and 0.11% on average. The maximal average increasing rate of the $\mathrm{PAD}_{0.25}$ was 0.86%. In contrast, Y decreased by only 5.61% at 5 L/min. Overall, the decreasing rate of silt increased with the increase in the flow discharge. The content of silt and the soil aggregate stability both decreased, but sand content increased under the three flow discharges.

There were no obvious changes in the soil structure of the new reconstructed purple soil with the increase in the slope length under erosion. However, the negative effect of erosion on the soil structure in the 10-m plot was serious. The maximal average reduction rate of silt (7.72%) and the maximal average increasing rate of sand (16.70%) both occurred in the 10-m plot. Meanwhile, the maximal average reduction rate of the MWD (25.18%) and the maximal average increasing rate

Table 4 Effects of flow discharge, slope length, and slope position on soil structure and their contributions based on ANOVA

Source	Sand		Silt		Clay		MWD		$\mathrm{PAD}_{0.25}$		Y	
	df	F	df	F	df	F	df	F	df	F	df	F
Flow discharge	3	0.05 NS	3	0.24 NS	3	1.81 NS	3	2.42 NS	3	13.05**	3	1.22 NS
Slope length	5	2.06 NS	5	1.74 NS	5	1.58 NS	5	3.80*	5	1.52 NS	5	3.21 NS
Slope position	2	3.67 NS	2	5.55 NS	2	1.19 NS	2	0.30 NS	2	0.97 NS	2	0.21 NS

*$p < 0.05$; **$p < 0.01$. *NS*, no significant ($p > 0.05$)

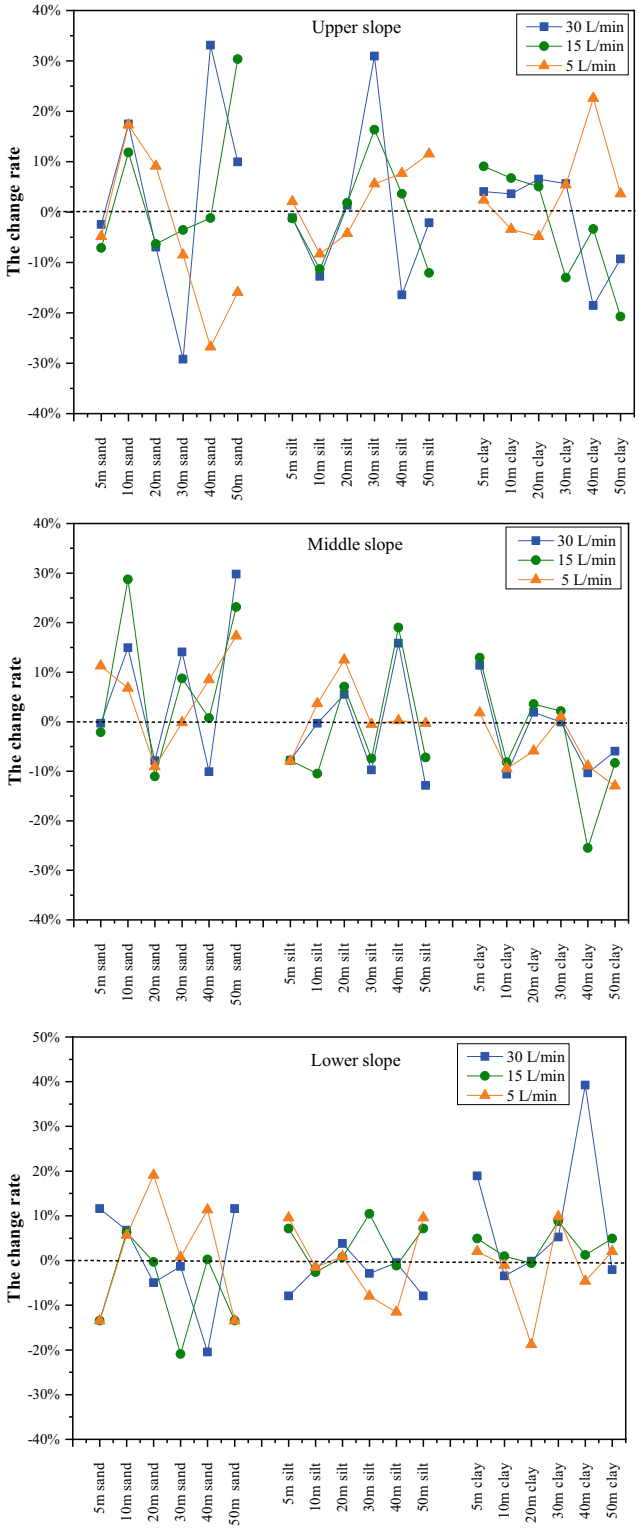

Fig. 3 Soil PSD variation in the topsoil before and after runoff scouring

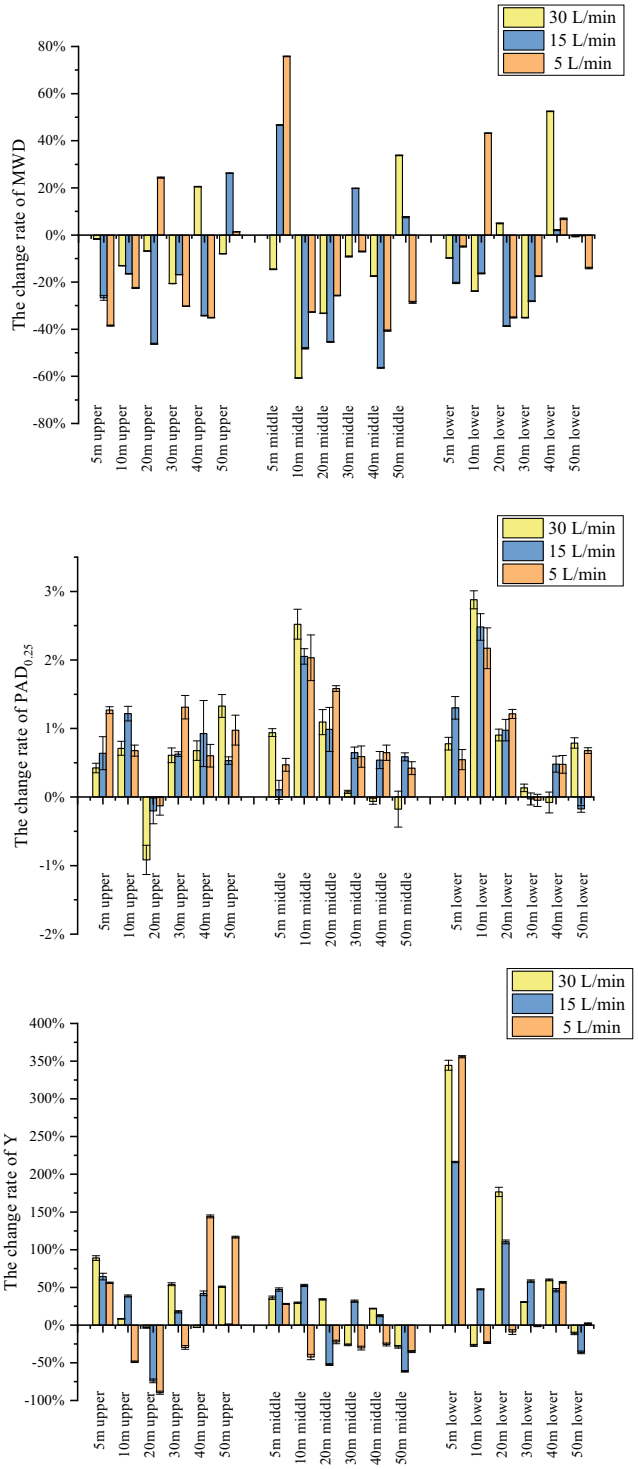

Fig. 4 Comparison of the soil aggregate stability index in the topsoil before and after runoff scouring

of the $PAD_{0.25}$ (1.86%) both occurred in the 10-m plot. The structure of the new reconstructed purple soil under the influence of the slope position on erosion was obviously different. The maximal average reduction rate of the MWD was 14.32% at the upslope position and the $\Delta PAD_{0.25}$ was 0.63%. Clay and sand particles showed an increase of 0.15% and 0.09%. The average silt and *Y* value decreased by 0.19% and 6.11%. At the middle slope position, the average clay and silt contents increased by 3.10% and 6.39%, respectively, while the

Table 5 The average change rates of soil PSD and aggregate stability under different flow discharges, slope lengths, and slope positions

Mean values (%)	The change rate of PSDs			The change rate of soil aggregate stability		
	Δclay (%)	Δsilt (%)	Δsand (%)	ΔMWD (%)	$\Delta PAD_{0.25}$ (%)	ΔY (%)
30 L/min	1.50	−2.11	1.27	−11.46	0.70	27.64
15 L/min	−0.80	−1.00	2.02	−20.23	0.76	9.52
5 L/min	−1.04	−0.11	1.11	−12.78	0.86	−5.61
5 m	9.55	−3.84	−4.55	−3.44	0.72	101.58
10 m	−4.08	−7.72	16.70	−25.18	1.86	4.09
20 m	−1.71	3.20	−2.35	−22.75	0.61	−31.16
30 m	2.82	2.66	−5.41	−17.85	0.43	12.85
40 m	−2.07	2.25	−0.73	−15.12	0.47	15.51
50 m	−5.40	−1.79	7.74	1.44	0.55	−14.77
Upper slope	0.15	−0.19	0.09	−14.32	0.63	−6.11
Middle slope	3.10	6.39	−10.06	−12.98	0.69	−13.00
Lower slope	5.11	−0.52	−3.75	−7.87	0.72	4.58

average sand content decreased by 10.06%. The average reduction rate of the MWD was 12.98%, and the increasing rate of the $PAD_{0.25}$ was 0.69%. The maximal average increase in Y was 13.00%. At the downslope position, changes to the Y value and clay particle content showed an average increase of 4.58% and 5.11%. The silt and sand contents continued to decrease by 0.52% and 3.75%. The minimal average reduction rate of the MWD was 7.87% and the maximal average increasing rate of the $PAD_{0.25}$ was 0.72%. Overall, the reduction rate of the MWD decreased gradually from the position of the upper, middle, and lower slopes and the trend of the $PAD_{0.25}$ was opposite. The upslope area showed the destruction of aggregates. The middle slope was the main sedimentary area of silt and the area of microaggregate destruction. Microaggregates and clay particles were deposited on the lower slope areas.

3.3 The correlation between the erosion rate and soil structural variables

With the average erosion rate as a reference series, and the indicators of the topsoil structural variables as a comparative series, gray correlation analysis was performed (Deng 1987). The results indicated that the degree of the response of changes in the topsoil structural parameters to the erosion rate was ranked in the following order: γ_{MWD} (0.50) > γ_{clay} (0.47) > γ_{sand} (0.41) > γ_{silt} (0.40) > γ_{Q} (0.37) > γ_{PAD} (0.26) > γ_{L} (0.21) > γ_{Y} (0.16). The response of the soil structural parameters to the erosion rate was correlated in the new reconstructed purple soil, with the ΔMWD having the most significant effect on the erosion rate and Δclay having the second-most significant effect. As shown in Fig. 5, based on the ΔMWD and erosion rate, the formulas for predicting the erosion rate as established by exponential correlation were $R^2 = 0.8187$ (30 L/min) and $R^2 = 0.6483$ (5 L/min).

4 Discussion

4.1 Influence of the overland flow discharge on the soil structure of erosion under new reconstructed purple soil

The flow discharge rate influenced the erosion of new reconstructed purple soil in the hilly area ($p < 0.05$) in this study. The rainfall or runoff amount and (or) intensity are commonly used to describe the degree of soil erosion (Meyer and Monke 1965; Peng et al. 2014; Prosdocimi et al. 2016). The average

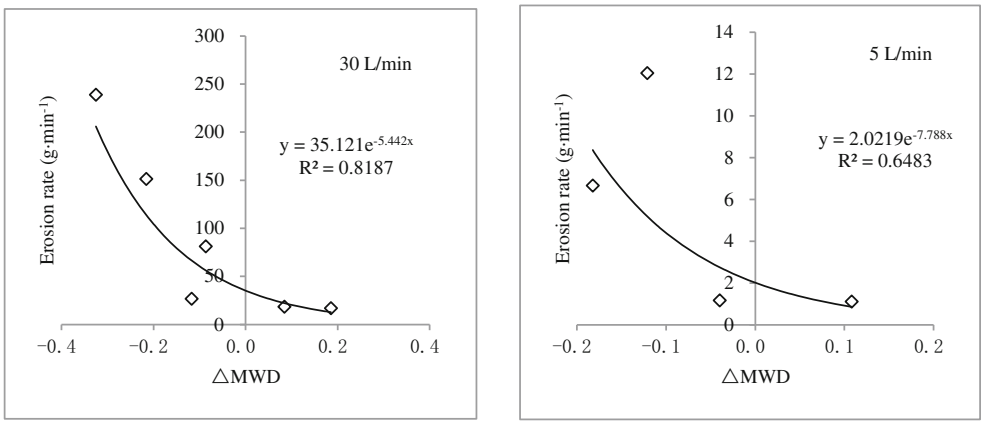

Fig. 5 Relationship between change rate of soil MWD (ΔMWD) and erosion rate on new reconstructed purple soil

erosion rate of new reconstructed purple soil increased with increasing flow discharge, which was consistent with the results of most studies (Hamed et al. 2002; Kang et al. 2016). First, the upper water inflow increased with the increase in the flow discharge, and the runoff of the slope soil increased per unit time. Therefore, the high surface runoff velocity increased the kinetic energy of erosion and the crushing capacity of soil particles in the new reconstructed purple soil.

Under different flow discharges, silt was preferentially eroded and soil aggregates were destroyed at 30 L/min, clay and silt were eroded simultaneously and the soil aggregate stability was damaged most seriously at 15 L/min, and clay loss was maximal and the macroaggregate were destroyed most severely at 5 L/min in our study. The microaggregates increased at 30 and 15 L/min, and the changes of the clay content were consistent with those of the microaggregates because clay is an important component of microaggregates (Bronick and Lal 2005) (Table 5). Previous studies showed that the destruction of soil macroaggregates was positively correlated with rainfall or runoff (Shen et al. 2008; Lu et al. 2016), which was not corroborated by our results. This difference may be explained by the influence of erosion on the soil PSD having priority under high flow discharge with the original PSDs of new reconstructed purple soil. Our study showed that the sand content increased under all three flow discharges, with the maximal increasing rate at 15 L/min (Fig. 3, Table 5). It was further shown that the destruction of aggregates was the source of sand particles, because the average maximal reduction rate of the MWD occurred at 15 L/min. Previous studies have also shown that PSDs after scouring were significantly coarser than those of the original soil (Chen et al. 2016; Ding and Huang 2017). This result can be explained by fine material being more easily transported than coarse material (Starr et al. 2000; Nadeu et al. 2010). We found that silt particles were the primary type of particles transported in the erosion of new reconstructed purple soil, as inferred from the increase in the decreasing rate of silt with the increase in the flow discharge matching that of the erosion rate. Additionally, the variation trends of silt and the $PAD_{0.25}$ with an increase in the flow discharge were contradictory (Table 5). This result showed that the silt loss was not from macroaggregates and was mainly from the soil matrix of the new reconstructed purple soil, which was different from the thought that macroaggregate breakdown is responsible for the production of fine materials (Le Bissonnais 2005; Shen et al. 2008). This is more likely attributable to the PSDs before scouring, in which the silt particle content was 36.69~43.05% in the new reconstructed purple soil (Table 2). This result is consistent with that of the high silt content having increased the soil erodibility due to its poor aggregation (Meyer et al. 1992). Refahi (2000) found that soils with 40~60% silt contents were the most vulnerable to erosion. Furthermore, purple soil particles develop from the fast weathering of siltstone, mudstone, and sandstone. In particular, the parent sedimentary rock environment of the Shaxi Miao Formation is a river with relatively dry conditions, leading to low organic matter and clay content (Wei et al. 2006; He et al. 2009). Additionally, Boonamnuayvitaya et al. (2004) indicated that particles less than 0.02 mm in diameter were particularly important for chemical transport, due to their large surface areas.

There was an exponential relationship between the ΔMWD and erosion rate when the flow discharge was 30 or 5 L/min as shown in Fig. 5, as the MWD increased the soil erosion resistance (Refahi 2000). This finding indicated that the soil aggregate stability properties of the new reconstructed purple soil were the main factors affecting the erosion rate under simulated high and low overland flow conditions. The large amount of water made the sediment and flow pattern more obvious; therefore, a high flow discharge increased the erosion intensity. This result agrees with the findings of Barthès and Roose (2002) and Fox et al. (2004), who clarified the effects of the water-stable aggregate and macroaggregate contents on the erosion amount by a negative correlation. In application of the models, some erosion models have begun to use the data of the soil structural characteristics as output or input parameters (Gholami et al. 2018). K is important for efficiently quantifying the soil erodibility efficiently in many models, having an obvious relationship with the soil particle-size distribution (PSD) and soil aggregate stability (Oztas and Fayetorbay 2003; Li et al. 2015).

4.2 Influence of the slope length and slope position on the soil structure of erosion under new reconstructed purple soil

The slope length is one of the key variables in empirical model of soil loss (Liu et al. 2000). This study found that changes of the soil structure were not obvious with the increase in the slope length; however, the damage to the soil PSD and aggregate stability in the 10-m plot was the worst (Table 5). Because the maximal average reduction rate of silt (7.72%) and the maximal average increasing rate of sand (16.70%) both occurred in the 10-m plot, these results showed that it was vulnerable to erosion. Additionally, the maximal average reduction rate of the MWD (25.18%) and the maximal average increasing rate of the $PAD_{0.25}$ (1.86%) both occurred in the 10-m plot due to its poor soil aggregate stability (Table 5). Meanwhile, the maximum values of the average erosion rates occurred in the 10-m plot when the flow rate was 30 L/min and 15 L/min (Table 3). The soil properties of the new reconstructed purple soil with a slope length of 10 m before souring showed poor aggregate stability and weak erosion resistance, such as the maximal silt content and the minimal $PAD_{0.25}$ both being in the 10-m plot before runoff scouring (Table 2). Additionally, the runoff shear stress, which causes soil particle

separation and sediment transport, was high in the 10-m plot at our experimental site (Zuo et al. 2018).

Our study showed that the destruction of the soil aggregate stability decreased gradually following the order of the upper to the middle and lower slopes, due to ΔMWD decreased gradually with the position of upper, middle, and lower slopes (Table 5). The upslope area showed intense destruction of aggregates. The mid-slope area was the main sedimentary area of silt and the area of microaggregate destruction. The lower slope areas were comprehensive depositional sites, in which microaggregates and clay particles were mainly deposited, and the reduction rates of the silt and sand contents in the lower slope areas were smaller than those in the middle slope areas (Fig. 3, Table 5). These results were different from those obtained for disturbed soil accumulation, in which clay and silt were transported mainly from the middle slope positions (Peng et al. 2014), but they were consistent with those obtained for other effects of human activities such as intense tillage (Chen et al. 2010). Generally, the runoff from the upper slope position increased in flow energy and velocity at the middle slope positions (Wang et al. 2004). Further, the middle slope position was the most complex location, where the process of deep excavation and filling coexisted with the process of farmland consolidation engineering. Soil transport and detachment coexisted at the middle slope position. Other studies have noted that clay particles were transported and deposited in large quantities to downhill positions (Chen et al. 2010). These results revealed that the soil aggregates were destroyed by erosion at all slope positions of the new reconstructed purple soil, with a variation tendency similar to those in the previous findings (Chen et al. 2010; Wei et al. 2017). However, the amplitude of change in this study was smaller than those in the others studies. Chen et al. (2010) reported that the $PAD_{0.25}$ increased maximally at the upper slope position in purple soil runoff plots (grade = 25°). This difference may be attributable to the gravity component of the water gravitational potential energy decreasing with a decrease in the slope gradient. The water gravitational potential energy of the 25° steep slope was larger than that of the 10° slope. The large slope gradient enhanced the runoff detachment and transport capacity and increased the soil aggregate loss (Poesen 1984). Furthermore, this study employed a field scouring experiment without the impact of raindrops and splash corrosion. In addition, the depth of the land and mechanical compaction can lead to changes in the structural profile of soil during the process of land consolidation. Although surface soil stripping and backfilling will greatly reduce this change, it is very difficult to produce uniform topsoil for backfilling (Wang et al. 2011). According to the above results of this research, soil and water conservation measures should be implemented on the upper slopes of new reconstructed purple soil with a slope length of 10 m which can effectively and economically control soil erosion. Soil PSD and MWD variables could be used as parameters for prediction of soil erosion on new reconstructed purple soil.

Although this experiment is only a case study, it is the first to explore the influence of the erosion on the soil structure of new reconstructed purple soil. Due to the limitations of experimental conditions, there are still some shortcomings in this experiment. The study is limited in that it involves only a single test of every experimental treatment. However, the analysis of this study mainly focuses on the effects of the flow discharge, slope length, and slope position on the soil structure in overland flow. Multiple sets of experimental data are collected under each influencing factor to ensure the accuracy of the results as much as possible. In addition, new reconstructed purple soil in the field is sensitive to natural rainfall. After experiencing the erosion from multiple rains over a period of time, new reconstructed purple soil will gradually change from the unsteady state to the stable state. To ensure the original state of the new reconstructed purple soil as much as possible, our experiment was completed within a short amount of time to reduce the impact of external environmental factors on the sample plot. Future work should focus, in particular, on the effects of artificial rainfall simulation on the soil structure and the fertility of the new reconstructed purple soil. Additionally, changes to the characteristics of the soil structure changing over time during erosion progression are essential for drawing comprehensive conclusions.

5 Conclusions

Erosion had significant and different effects on the soil PSD and aggregate stability of new reconstructed purple soil in overland flow under different flow discharges, slope lengths, and slope positions. (1) Silt was the primary particle transported during the erosion, and the decreasing rate of silt increased with the increase in the flow discharge. Silt was eroded most at 30 L/min, clay and silt were eroded simultaneously, and the soil aggregate stability was damaged most seriously at 15 L/min; clay loss was maximal and the macroaggregate were destroyed most severely at 5 L/min. The average erosion rates of new reconstructed purple soil increased with increasing flow discharge. The relationship between the erosion rate and ΔMWD was significantly exponential under high and low overland flow discharges. (2) The damage to the soil PSD and aggregates stability of the 10-m plot was the worst. The silt and MWD maximally decreased by 7.72% and 1.86%, and the sand and $PAD_{0.25}$ maximally increased by 16.70% and 25.18%, which all occurred in the 10-m plot. (3) The destruction of the soil aggregate stability decreased gradually following the order of the upper to the middle and lower slopes. The upslope showed intense destruction of aggregates. The middle slope was the main sedimentary area of silt and the area of microaggregate destruction. The lower slope areas were comprehensive depositional sites, in which

microaggregates and clay particles were mainly deposited, and the reduction rates of the silt and sand content were smaller than those in the middle slope. Hence, it is better to implement soil and water conservation measures on the upper slope of new reconstructed purple soil with a slope length of 10 m which can effectively and economically control soil erosion. The soil PSD and MWD variables could be used as parameters for the prediction of soil erosion in new reconstructed purple soil.

Funding information This work was financially supported by the National Natural Science Foundation of China (NSFC: 41730854, 91425301), Ten Thousand Talent Program for leading young scientist, and the state key development program in China "Constructing an efficient ecological interception technology system by combining source reduction,-biological isolation and-wetland disposal" (2017YFD0800505).

References

Ampontuah EO, Robinson JS, Nortcliff S (2006) Assessment of soil particle redistribution on two contrasting cultivated hillslopes. Geoderma 132:324–343

Asadi H, Moussavi A, Ghadiri H, Rose CW (2011) Flow–driven soil erosion processes and the size selectivity of sediment. J Hydrol 406:73–81

Barthès B, Roose E (2002) Aggregate stability as an indicator of soil susceptibility to runoff and erosion; validation at several levels. Catena 47:133–149

Boonamnuayvitaya V, Chaiya C, Tanthapanichakoon W, Jarudilokkul S (2004) Removal of heavy metals by adsorbent prepared from pyrolyzed coffee residues and clay. Sep Purif Technol 35:11–22

Bronick CJ, Lal R (2005) Soil structure and management: a review. Geoderma 124:3–22

Cerdà A, Bodí MB, Hevilla-Cucarella E (2007) Erosión del suelo en plantaciones de cítricos en ladera. Valle del riu Canyoles, Valencia. Agroecología 2:85–91

Chen XY, Niu QX, Zhou J, Wei CF, Xie DT, He BH (2010) Study on spatial variability characters of steep purple soil particles under rainfall simulation condition. J Soil Water Conserv 24(5):163–168

Chen SN, Ai XY, Dong TY, Li BB, Luo RH, Ai YW, Chen ZQ, Li CR (2016) The physico-chemical properties and structural characteristics of artificial soil for cut slope restoration in Southwestern China. Sci Rep 6:20565

Chongqing Land Development and Consolidation Project Construction Standard (Trial) (2007)

Curtaz F, Stanchi S, D'Amico ME, Filippa G, Zanini E, Freppaz M (2015) Soil evolution after land-reshaping in mountains areas (Aosta Valley, NW Italy). Argic Ecosyst Environ 199:238–248

Deng JL (1987) Grey system basic method. Huazhong University of Science and Technology Press, Wuhan, pp 17–34

Ding W, Huang C (2017) Effects of soil surface roughness on interrill erosion processes and sediment particle size distribution. Geomorphology 295:801–810

FAO/Unesco (1988) Soil map of the world, revised legend. FAO, Rome

Fiès JC, Bruand A (1998) Particle packing and organization of the textural porosity in clay-silt-sand mixtures. Eur J Soil Sci 49:557–567

Fox DM, Bryan RB, Fox CA (2004) Changes in pore characteristics with depth for structural crusts. Geoderma 120:0–120

Gholami V, Booij MJ, Nikzad Tehrani E, Hadian MA (2018) Spatial soil erosion estimation using an artificial neural network (ANN) and field plot data. Catena 163:210–218

Hamed Y, Jean A, Pepin Y, Asseline J, Nasri S, Zante P, Berndtsson R, El-Niazy M, Balah M (2002) Comparison between rainfall simulator erosion and observed reservoir sedimentation in an erosion-sensitive semiarid catchment. Catena 50:1–16

Hao HX, Wang JG, Guo ZL, Hua L (2019) Water erosion processes and dynamic changes of sediment size distribution under the combined effects of rainfall and overland flow. Catena 173:494–504

He XB, Bao YH, Nan HW, Xiong DH, Wang L, Liu YF, Zhao JB (2009) Tillage pedogenesis of purple soils in southwestern China. J Mt Sci 6:205–210

Kang HL, Wang WL, Xue ZD, Guo MM, Shi QH, Li JM, Guo JQ (2016) Erosion morphology and runoff generation and sediment yield on ephemeral gully in loess hilly region in field scouring experiment. Transactions of the Chinese Society of Agricultural Engineering 32: 161–170 (in Chinese)

Kara O, Sensoy H, Bolat I (2010) Slope length effects on microbial biomass and activity of eroded sediments. J Soils Sediments 10: 434–439

Kosmas C, Gerontidis ST, Marathianou M, Detsis B, Zafiriou TH, Muysen WN, Govers G, Quine T, Vanoost K (2001) The effects of tillage displaced soil on soil properties and wheat biomass. Soil Tillage Res 58:31–44

Le Bissonnais Y (2005) Aggregate breakdown mechanisms and erodibility. Encyclopedia of soil science CRC Press pp 40–44

Li ZW, Zhang GH, Geng R, Wang H (2015) Spatial heterogeneity of soil detachment capacity by overland flow at a hillslope with ephemeral gullies on the Loess Plateau. Geomorphology 248:264–272

Liao YS, Cai QG, Cheng QJ (2008) Critical topographic condition for slope erosion in hilly-gully region of Loess Plateau. Science of Soil and Water Conservation 6:32–38

Liu J (2015) Soil engineering effect of farming plots reconstruction in hilly–mountainous region of Chongqing. PhD thesis, Southwest University (in Chinese)

Liu BY, Nearing MA, Shi PJ, Jia ZW (2000) Slope length effects on soil loss for steep slopes. Soil Sci Soc Am J 64:1759–1763

Liu J, Du J, Wei C, Zhong M, Liu B (2015) Effects of land consolidation period of farmland on soil properties in purple region. Transactions of the Chinese Society of Agricultural Engineering 31:254–261 (in Chinese)

López-Tarazón JA, Batalla RJ, Vericat D, Balasch JC (2010) Rainfall, runoff and sediment transport relations in a mesoscale mountainous catchment: the river Isábena (Ebro basin). Catena 82:23–34

Lu J, Zheng F, Li G, Bian F, An J (2016) The effects of raindrop impact and runoff detachment on hillslope soil erosion and soil aggregate loss in the mollisol region of northeast China. Soil Tillage Res 161: 79–85

Meyer LD, Monke EJ (1965) Mechanics of soil erosion by rainfall and overland flow. Trans ASAE 8:572–580

Meyer LD, Line DE, Harmon WC (1992) Size characteristics of sediment from agricultural soils. J Soil Water Conserv 47:107–111

Nadeu E, Boix-Fayos C, De Vente J, López J, Martínez-Mena M (2010) Organic carbon mobilization by different erosive processes in the slope-channel connection. Movilización de carbono orgánico por distintos procesos erosivos en la conexión laderacauce. Pirineos 165:157–177

Oades JM, Waters AG (1991) Aggregate hierarchy in soils. Aust J Soil Res 29:815–828

Oztas T, Fayetorbay F (2003) Effect of freezing and thawing processes on soil aggregate stability. Catena 52:1–8

Peng XD, Shi DM, Dong J, Wang SS, Li YX (2014) Runoff erosion process on different underlying surfaces from disturbed soils in the Three Gorges Reservoir Area, China. Catena 123:215–224

Piccarreta M, Faulkner H, Bentivenga M, Bentivengac M, Capolongo D (2006) The influence of physico-chemical material properties on erosion processes in the badlands of Basilicata, Southern Italy. Geomorphology 81:235–251

Poesen J (1984) The influence of slope angle on infiltration rate and Hortonian overland flow. Z. Geomorphol., Supplement Band 49: 117–131

Prosdocimi M, Cerdà A, Tarolli P (2016) Soil water erosion on Mediterranean vineyards: a review. Catena 141:1–21

Ramos MC, Cots-Folch R, Martínez-Casasnovas JA (2007) Effects of land terracing on soil properties in the Priorat region in northeastern Spain: a multivariate analysis. Geoderma 142:251–261

Refahi HGh (2000). Water erosion and conservation. Tehran University Press, pp. 551 (in Persian)

Shen Y, Zhang XP, Liang AZ, Li WF, Yang XM (2008) Study on properties of soil loss from sloping farmland of black soil based on a runoff event. Agric Res Arid Areas 26:224–229 (in Chinese)

Shi ZH, Fang NF, Wu FZ, Wang L, Yue BJ, Wu GL (2012) Soil erosion processes and sediment sorting associated with transport mechanisms on steep slopes. J Hydrol 454:123–130

Six J, Elliott ET, Paustian K (2000) Soil structure and soil organic matter II. A normalized stability index and the effect of mineralogy. Soil Sci Soc Am J 64:1042–1049

Sklenicka P (2006) Applying evaluation criteria for the land consolidation effect to three contrasting study areas in the Czech Republic. Land Use Policy 23:502–510

Starr GC, Lal R, Malone R, Hothem D, Owens L, Kimble J (2000) Modeling soil carbon transported by water erosion processes. Land Degrad Dev 11:83–91

Stomph TJ, Ridder N, Steenhuis TS, Giesen NCVD (2002) Scale effects of Hortonian overland flow and rainfall-runoff dynamics: laboratory validation of a process-based model. Earth Surf Process Landf 27: 847–855

Thomaz EL (2018) Interaction between ash and soil microaggregates reduces runoff and soil loss. Sci Total Envrion 625:1257–1263

Tian X, Gao K, Zhang LJ, Yu YQ, Han GD (2015) Effect of slope position on spatial distribution of soil water and vegetation in sandy land. Bulletin of Soil and Water Conservation 35:12–16 (in Chinese)

Wakindiki IIC, Ben–Hur M (2002) Soil mineralogy and texture effects on crust micromorphology, infiltration, and erosion. Soil Sci Soc Am J 66:897–905

Wang WL, Lei AL, Li ZB, Tang KL (2004) Numerical simulation of multiple submerged jets on multilevel dicharged into plunge pool. J Hydraul Eng 35:25–30 38

Wang AL, Zhao GX, Wang QF, Liu WP (2011) Effects of land consolidation on soil physical and chemical characteristics of hilly region. Transactions of the Chinese Society of Agricultural Engineering 27: 311–315

Wang L, Shi ZH, Wang J, Fang NF, Wu GL, Zhang HY (2014) Rainfall kinetic energy controlling erosion processes and sediment sorting on steep hillslopes: a case study of clay loam soil from the Loess Plateau, China. J Hydrol 512:168–176

Wang Y, Ran L, Fang N, Shi Z (2018) Aggregate stability and associated organic carbon and nitrogen as affected by soil erosion and vegetation rehabilitation on the Loess Plateau. Catena 167:257–265

Wei CF, Xie DT, Yang JH, Wang QK, He JL (1994) Study on soil fertility evolution of purple hilly sloping land. Mountain development 5:61–66

Wei CF, Gao M, Che FC, Qu M, Yang JH, Xie DT (2000) Study on the fertility characteristics of soils in immigration's reclamation area of ErTan hydropower station. Acta Pedol Sin 27:536–544

Wei CF, Ni JP, Gao M, Xie DT, Hasegawa S (2006) Anthropic pedogenesis of purple rock fragments in Sichuan Basin, China. Catena 68: 51–58

Wei S, Zhang X, McLaughlin NB, Chen X, Jia S, Liang A (2017) Impact of soil water erosion processes on catchment export of soil aggregates and associated SOC. Geoderma 294:63–69

Wu XL, Wei YJ, Wang JG, Xia JW, Cai CF, Wu LL, Fu ZY, Wei ZY (2017) Effects of erosion degree and rainfall intensity on erosion processes for Ultisols derived from quaternary red clay. Agric Ecosyst Environ 249:226–236

Xie JQ, Tang CJ, Li XW (2005) China's sloping farmland. Beijing. China Earth Press 29–31:49–55 (in Chinese)

Xu C, Gao M, Xie DT, Jiang T, Li S, Wei CF (2009) Effect of land consolidation history on soil quality of purple hilly region. Transactions of the Chinese Society of Agricultural Engineering 25:242–248 (in Chinese)

Yu G, Feng J, Che Y, Lin X, Hu L, Yang S (2010) The identification and assessment of ecological risks for land consolidation based on the anticipation of ecosystem stabilization: a case study in Hubei province, China. Land Use Policy 27:293–303

Zhang P, Wei T, Jia Z, Han Q, Ren X (2014) Soil aggregate and crop yield changes with different rates of straw incorporation in semiarid areas of northwest China. Geoderma 230–231:41–49

Zheng BZ (2013) Technical guide to soil analysis. Beijing, pp 36–37

Zuo FL, Zhong SQ, Ran ZL, Wei CF (2018) Characteristics of sediment and hydrodynamic parameters of new reconstructed slope soil in the hill area with purple soils. J Soil Water Conserv 32:59–66 (in Chinese)